coatings

MDPI

Article

Polypyrrole-Coated Melamine Sponge as a Precursor for Conducting Macroporous Nitrogen-Containing Carbons

Jaroslav Stejskal [1,*], Jarmila Vilčáková [2,3], Marek Jurča [2], Haojie Fei [2], Miroslava Trchová [4], Zdeňka Kolská [5], Jan Prokeš [6] and Ivo Křivka [6]

1 Institute of Macromolecular Chemistry, Academy of Sciences of the Czech Republic, 162 06 Prague 6, Czech Republic
2 Centre of Polymer Systems, Tomas Bata University in Zlin, 760 01 Zlin, Czech Republic; vilcakova@utb.cz (J.V.); jurca@utb.cz (M.J.); haojie@utb.cz (H.F.)
3 Polymer Centre, Faculty of Technology, Tomas Bata University in Zlin, 760 01 Zlin, Czech Republic
4 Central Laboratories, University of Chemistry and Technology, Prague, 166 28 Prague 6, Czech Republic; Miroslava.Trchova@vscht.cz
5 Faculty of Science, J. E. Purkyně University, 400 96 Ústí nad Labem, Czech Republic; Zdenka.Kolska@ujep.cz
6 Faculty of Mathematics and Physics, Charles University, 180 00 Prague 8, Czech Republic; jprokes@semi.mff.cuni.cz (J.P.); krivka@semi.mff.cuni.cz (I.K.)
* Correspondence: stejskal@imc.cas.cz

Abstract: Macroporous open-cell melamine sponges were coated with a conducting polymer, polypyrrole, during in-situ oxidative polymerization of pyrrole. Two samples, differing in polypyrrole content, 8.2 and 27.4 wt%, were prepared. They were exposed to various temperatures up to 700 °C in an inert atmosphere. The macroporous structure and mechanical integrity were preserved after this process. This converted both the polypyrrole coating and the melamine sponge to macroporous nitrogen-containing carbons. The changes in molecular structure in the course of carbonization were followed by elemental analysis and FTIR and Raman spectra. The specific surface area of polypyrrole-coated sponge increased from ca. 90 to ca. 300 $m^2\ g^{-1}$ along with accompanying increase in the porosity. The conductivity of the sponges was recorded as a function of compression in a newly developed apparatus. The sponge containing 27.4 wt% pyrrole had conductivity of the order of 10^{-2} S·cm^{-1} at 0.1 MPa pressure, which was reduced by four orders of magnitude when exposed to 400–500 °C and nearly recovered after the temperature reached 700 °C. The sponges were tested in electromagnetic radiation shielding and displayed both radiation absorption and, to a lower extent, radiation reflection proportional mainly to the samples' conductivity.

Keywords: conducting polymer; polypyrrole; carbonization; nitrogen-containing carbon; macroporous conducting sponge

Citation: Stejskal, J.; Vilčáková, J.; Jurča, M.; Fei, H.; Trchová, M.; Kolská, Z.; Prokeš, J.; Křivka, I. Polypyrrole-Coated Melamine Sponge as a Precursor for Conducting Macroporous Nitrogen-Containing Carbons. *Coatings* **2022**, *12*, 324. https://doi.org/10.3390/coatings12030324

Academic Editor: Arūnas Ramanavičius

Received: 21 January 2022
Accepted: 25 February 2022
Published: 1 March 2022

1. Introduction

Melamine sponge is a macroporous material based on a melamine-formaldehyde network containing some bisulfite moieties [1]. Melamine alone is an organic compound, rich both in nitrogen and carbon (Figure 1a), which makes it a suitable precursor for carbonization. It has been exposed to elevated temperature in an inert atmosphere to obtain materials that were regarded as carbons [2–5], nitrogen-containing carbons [4,6], or products close to carbon nitrides [7]. Except for some shrinkage, the macroporous morphology of the sponges was preserved after carbonization [4], but the mechanical properties were poor. Carbonized macroporous melamine sponges have been proposed as adsorbents of organic chemicals [2,3], e.g., in the treatment of oil spills [8,9]. They served as flexible supercapacitor electrodes [2,10–12], or in strain sensing [5].

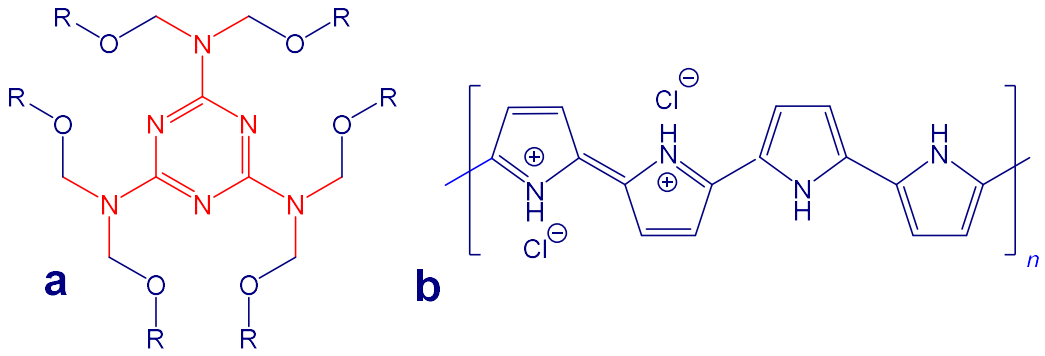

Figure 1. The molecular structure of (**a**) melamine/formaldehyde constituting the sponge, and (**b**) polypyrrole salt (hydrochloride). The melamine moiety is depicted in red; R = H or a linkage to another melamine unit.

Conducting polymers, such as polyaniline and polypyrrole (Figure 1b), are similarly composed mainly of carbon and nitrogen atoms. They have been used frequently for the preparation of nitrogen-enriched carbons by exposure to elevated temperature in an inert atmosphere [13]. The carbonization of various polypyrrole nanostructures—globules, nanofibers and nanotubes—provides nitrogen-containing carbons of various morphology [14] with conductivity at the semiconductor level. The general features of morphology do not change after carbonization and, for example, polypyrrole globules or nanotubes convert to nitrogen-enriched carbon analogues [14,15].

Macroporous polymer materials have been coated with conducting polymers in studies conducted many years ago [16,17], as well as in more recent reports [18,19]. Melamine sponge can be modified in a similar manner with the conducting polymers, polyaniline [20–22] and polypyrrole [6,23–27]. For example, melamine sponge coated with polyaniline was used for mass-spectrometric monitoring of perfluorooctane compounds [22] and for oil absorption [20]. The systems developed based on polypyrrole have generally included additional components. Sponge coated with polypyrrole combined with dopamine and carbon nanotubes was used to reduce the oil viscosity in spills by Joule heating generated by passing a current [26]. The deposition of polypyrrole on melamine sponge with adsorbed graphene [23], graphene oxide [25] or incorporated carbon fibres [24] produced compressible supercapacitor electrodes. The single-step coating of melamine sponge with polypyrrole and magnetite generated a ferrosponge suitable for microwave radiation shielding [27].

It is an obvious strategy to combine melamine and conducting polymers in the preparation of carbonaceous analogues. While the former component will affect mechanical properties, the latter will control electrical properties. The authors are aware of only a single study in which melamine sponge was coated with polyaniline and subsequently carbonized at 600–800 °C to obtain supercapacitor electrodes [21]. For the sake of completeness, the coating of a carbonized melamine sponge with polyaniline should also be mentioned [5,28].

In the present study, a commercial macroporous melamine sponge coated with polypyrrole was exposed to various temperatures up to 700 °C and the properties of the products were analyzed. Attention was paid especially to electrical properties. The selection of the system was based on the observations that the sponges maintain a macroporous structure after carbonization [8], and that carbonized polypyrrole retains a reasonable level of conductivity [14]. These sponges represent a new class of carbonaceous materials which could be considered for use in various applications, especially in energy-storage devices, such as supercapacitors. Other potential uses, illustrated here by electromagnetic radiation shielding, are also presented in the report.

2. Experimental Methods

2.1. Synthesis and Carbonization

Open-cell macroporous melamine/formaldehyde Basotect (BASF AG, Ludwigshafen, Germany) sponges, advertised as "miraculous cleaning sponges", of 105 mm × 62 mm ×

25 mm size were purchased from Drogerie ZDE (Prague, Czech Republic). The sponges were immersed in a freshly prepared aqueous mixture, in which 0.025 M pyrrole was oxidized with 0.0625 M iron (III) chloride hexahydrate (both chemicals of reagent grade >98%; Sigma Aldrich, St. Louis, MO, USA) at ambient temperature. The sponges were squeezed to replace air in the pores with an aqueous phase. The polymerization of pyrrole was complete within several minutes but the sponges were left in the reaction medium at rest for 1 h. The sponges were then transferred into an excess of 0.2 M hydrochloric acid and washed until no dark precipitate was released. The sponges were then moved to ethanol to remove water from macropores, ethanol was exchanged several times, and finally the sponges were left to dry in open air. The content of polypyrrole was calculated from the mass increase. Polypyrrole powder generated outside the sponges was also collected and treated in the same manner.

Low concentrations of pyrrole and oxidant were selected to slow down polymerization and to promote polypyrrole coating at the expense of formation of polypyrrole precipitate in the macropores. However, because the polypyrrole content of the coated sponge was also relatively low at 8.2 wt%, in the following experiment the concentrations of both pyrrole and oxidant were doubled and the polypyrrole content was increased to 27.4 wt%.

The polypyrrole-coated sponges were subsequently placed in a tube furnace GSL-1600X-50-UL (MTI Corp., Richmond, CA, USA) and heated under an argon atmosphere at 3 °C·min^{-1} rate to target temperature up to 700 °C. The power was switched off and the samples were left to cool under an inert atmosphere. The difference between the original and residual weight of sponges after the exposure, i.e., the carbonization yield, was determined.

2.2. Characterization

Morphology was assessed with a scanning ultra-high-resolution electron microscope MAIA3 Tescan. Elemental composition was determined using a Perkin Elmer 2400 Series II CHNS/O Analyzer.

FTIR spectra were collected using a Nicolet 6700 spectrometer (Thermo Fisher Scientific, Madison, WI, USA) equipped with reflective ATR extension GladiATR (PIKE Technologies, Fitchburg, WI, USA) with a diamond crystal. Spectra were recorded in the 4000–400 cm^{-1} range at resolution 4 cm^{-1}, after 64 scans and Happ–Genzel appodization.

Raman spectra were recorded with a Thermo Scientific DXR Raman microscope operating with a 780 nm laser line and 4 mW power. The spot size of the laser was focused by 50× objective lens. The scattered light was analyzed by a spectrograph with holographic gratings of 1200 lines mm^{-1} and a pinhole width of 50 μm. The acquisition time was 10 s with 10 repetitions.

The specific surface area and pore volume were determined from the adsorption and desorption isotherms with a NOVA3200 analyzer (Quantachrome Corp., Boynton Beach, FL, USA) using NovaWin software. The samples were degassed for 24 h at 100 °C, then adsorption and desorption isotherms were recorded with nitrogen (Linde Gas, a.s., Prague, Czech Republic, 99.999%). Five-point Brunauer–Emmett–Teller (BET) analysis was applied for total surface area determination and the 40-point Barrett–Joyner–Halenda model for pore volume.

2.3. Conductivity and Mechanical Properties

The conductivity of the sponges was determined using the four-point van der Pauw method in a laboratory-designed apparatus (Figure 2) composed of a cylindrical glass cell with an inner diameter of 10 mm. The sponges were placed between an insulating glass support and a glass piston carrying four platinum/rhodium electrodes at the perimeter of its base. The setup used a Keithley 220 programmable current source, a Keithley 2010 multimeter and a Keithley 705 scanner with a Keithley 7052 matrix card. The pressure up to 10 MPa applied to the sample was measured using a L6E3 strain gauge cell (Zemic Europe BV, Etten-Leur, The Netherlands). The signal of the strain gauge resistance bridge was

converted to direct voltage by a TZA31400 converter (ATERM, Pohořelice, Czech Republic). The voltage was measured with a Keithley 195A multimeter. Force was applied using an E87H4-B05 stepper motor with 200 steps per revolution (Haydon Switch & Instrument Inc., Waterbury, CT, USA), which acts on the upper glass piston of the apparatus via a helical gear with a pitch of 0.016 mm per step. The actual thickness of the measured sample must be known to determine the resistivity, therefore the tip of a dial indicator Mitutoyo IDC 543-122FB (Mitutoyo s.r.o., Teplice, Czech Republic) rests on the upper side of the glass piston, by means of which the change in sample thickness can be continuously recorded.

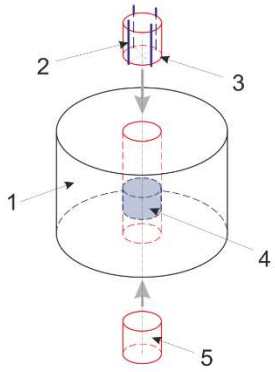

Figure 2. Four-point method of conductivity determination: 1—glass cylinder, 2—platinum/rhodium contact wires, 3—glass piston with incorporated platinum electrodes, 4—sponge, 5—glass support.

2.4. Electromagnetic Radiation Shielding

The electromagnetic radiation shielding parameters of the sponges were studied with a PNA-L Network Analyzer Agilent N5230A (Agilent Technologies, Santa Clara, CA, USA) in the frequency X-band, WR90 (8.2–12.4 GHz). The details of the experimental procedure and data evaluation have been reported previously [27].

3. Results and Discussion

3.1. Carbonization Concept

The carbonization of polypyrrole powders was earlier studied in detail for various morphologies, such as globular polypyrrole and polypyrrole nanofibers and nanotubes [14]. The process had three distinct phases. When exposed to 200–300 °C, conducting polypyrrole salts (Figure 1b) became deprotonated to polypyrrole bases with consequent decrease in conductivity [29]. The further elevation of temperature to 400 °C caused the degradation of polymer chains and loss of conjugation with associated conductivity decrease to insulating level. The conductivity gradually recovered at a still higher temperature in response to continuing carbonization. It was assumed that a similar scenario would also be applicable to polypyrrole composites, here polypyrrole deposited on melamine sponges, which is considered in subsequent discussion. While previous studies have been performed on intractable polypyrrole powders [14], the present study concerned a macroporous compressible conducting composite that can be applied in various directions.

3.2. Carbonization Course

Exposure of sponges to elevated temperatures was associated with a decrease in mass (Figure 3). When heated in an inert atmosphere, the initial decrease at 200–300 °C corresponded to the release of moisture and hydrochloric acid from polypyrrole hydrochloride (Figure 1b). The neat melamine sponge left a 10 wt% residue at 700 °C. This is rather low for the practical preparation of a carbonaceous material. Polypyrrole alone is known to leave a residue above 50 wt% [14]. The yield therefore improved after the sponge was coated with polypyrrole. The results are important for the application of conducting sponges as materials heated by Joule heat produced by passing an electrical current [6,14,26,30].

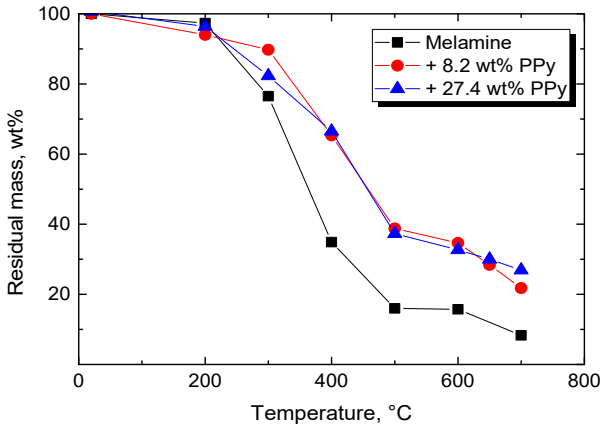

Figure 3. The residual mass of melamine sponge (black squares) and polypyrrole-coated melamine sponges after exposure to elevated temperature.

3.3. Morphology

The threads in the melamine sponge became coated with a compact polypyrrole film with some adhering polypyrrole globules and their clusters (Figure 4a). Based on previous studies comparing the uncoated and polypyrrole-coated sponges, the polypyrrole shell was estimated be of submicrometre thickness [30]. It had already been established that the morphology did not change after carbonization (Figure 4b) [13], except for a minute shrinkage observable only on macroscopic samples.

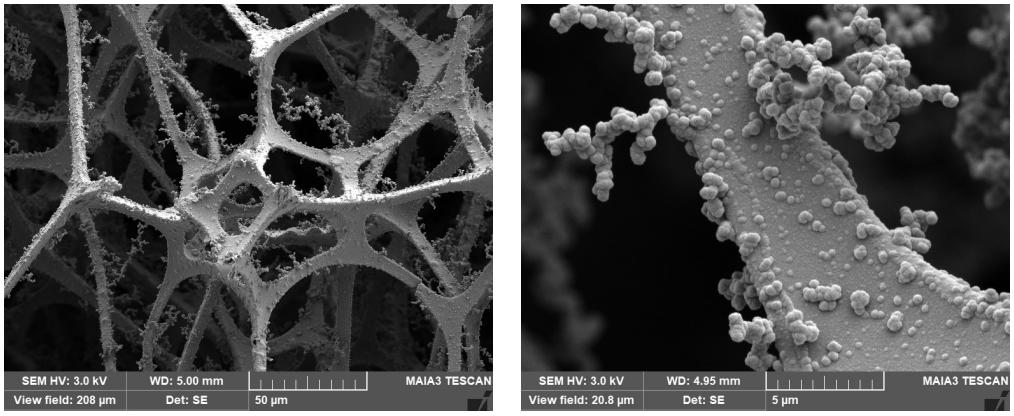

(**a**) Polypyrrole/melamine

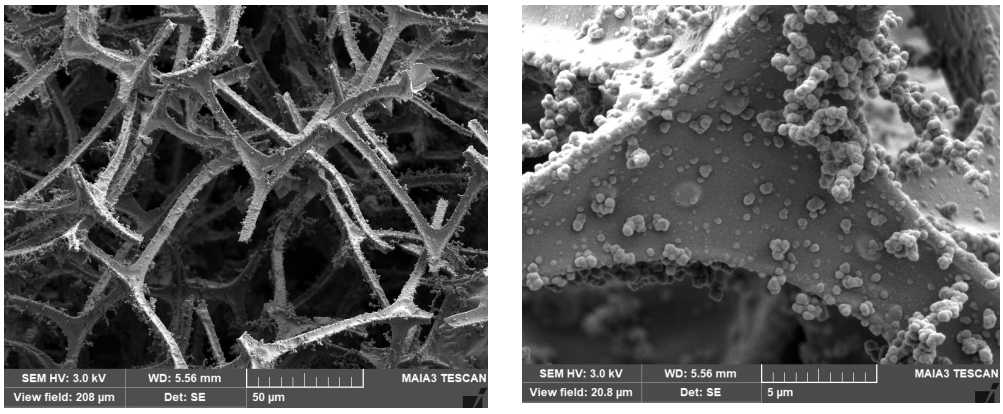

(**b**) Polypyrrole/melamine—carbonized at 650 °C

Figure 4. Micrographs of polypyrrole-coated melamine sponge (**a**) before, and (**b**) after carbonization at 650 °C taken at lower (**left**) and higher magnification (**right**).

3.4. Elemental Composition

The term carbonization implies that the carbon content should increase during this process, which was indeed the case for both polypyrrole-coated sponges (Figure 5). Yet, the samples contained a significant fraction of nitrogen, which was gradually reduced in the course of carbonization. The presence of lone electron pairs on nitrogen atoms is beneficial in applications involving adsorption phenomena, such as in electrodes in supercapacitors, or dye removal in water-pollution treatment, and also in heterogeneous catalysis. The atomic C/N ratio thus grew as the carbonization temperature increased (Figure 6). The hydrogen content was reduced, and most likely released, along with some oxygen, as water. The presence of oxygen in the samples derives mainly from formaldehyde links in melamine (Figure 1a), but it is known also to be present in polypyrrole [13,14]. The marked increase in oxygen content above 400 °C was observed only for neat melamine sponge (Figure 5, black squares) but not for the carbonized composites with polypyrrole, which can still be considered as nitrogen-containing carbons. The trends in the evolution of elemental composition were in accordance with an earlier study on neat polypyrrole powders [14]. It should be noted that the original composites also contained chlorine counter-ions in polypyrrole (Figure 1b), which were released as hydrochloric acid in the early stages of carbonization.

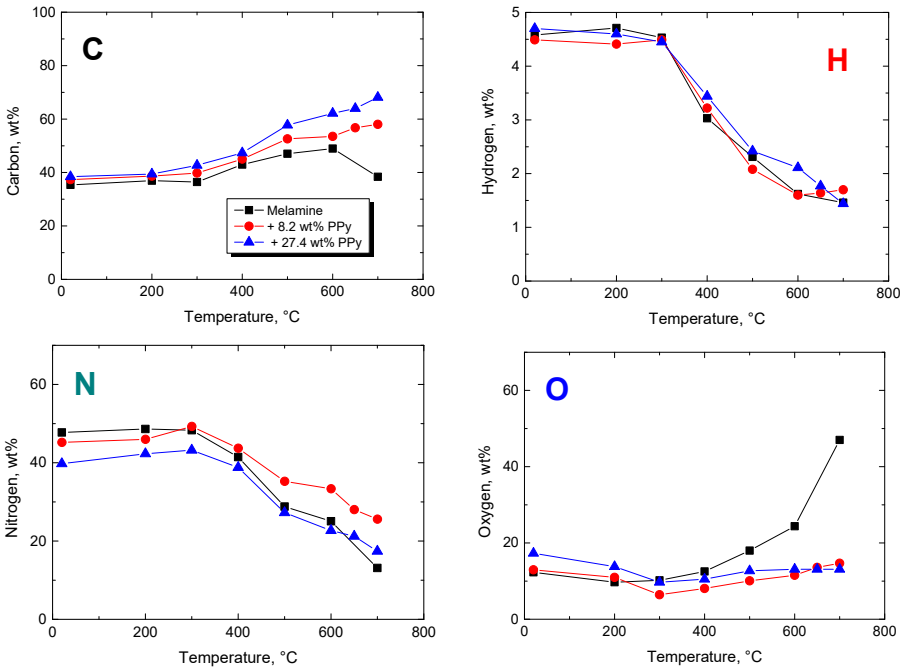

Figure 5. The composition of sponges exposed to various temperatures obtained by elemental CHN analysis; oxygen (including some chlorine) content was calculated as a residue.

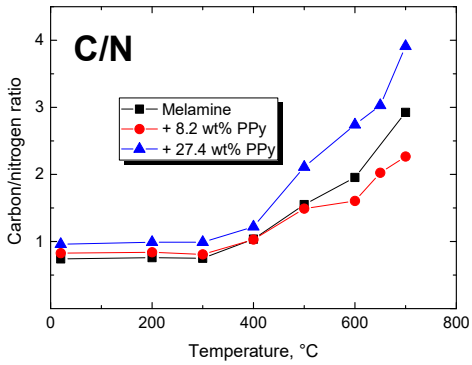

Figure 6. The dependence of carbon-to-nitrogen atomic ratio on the carbonization temperature.

3.5. FTIR Spectroscopy

The ATR FTIR spectra of neat melamine sponge remained unchanged until the temperature reached approximately 300 °C (Figure 7a). The main bands were detected in the spectra with local maxima at 1540, 1447, 1323, 878, 744 cm^{-1} and a sharp peak at 805 cm^{-1}. At approximately 400 °C, the spectra were transformed into two broad bands with maxima at approximately 1578 and 1269 cm^{-1}, while the sharp peak was shifted to 837 cm^{-1}. At 700 °C the spectrum exhibited two broad bands with maxima at 1578 and 1123 cm^{-1}, with some small peaks at 1728, 1450 and 837 cm^{-1}. We infer that the infrared spectra reflect a structural transformation of melamine sponge which takes place at about 400 °C.

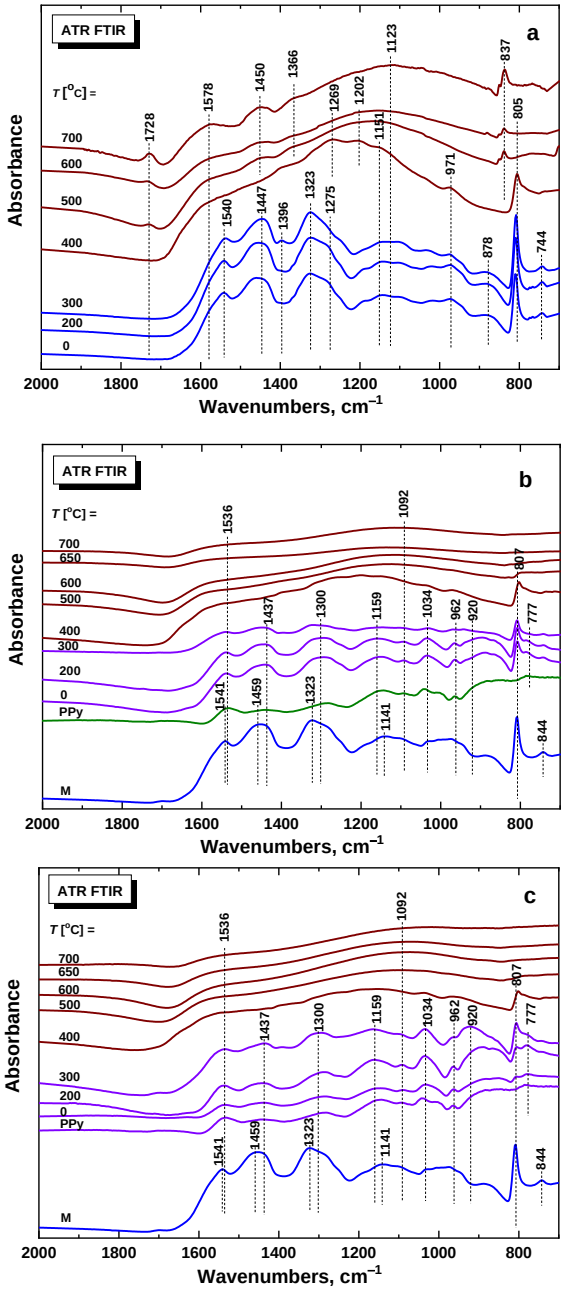

Figure 7. The evolution of the ATR FTIR spectra of (**a**) the melamine sponge (M), (**b**) the melamine sponge containing 8.2 wt%, and (**c**) 27.4 wt% polypyrrole, after exposure to various temperatures in inert atmosphere. Polypyrrole (PPy) spectrum is included for comparison. The groups of similar spectra are distinguished by colors.

In the ATR FTIR spectra of the melamine sponge coated with polypyrrole (Figure 7b,c), we observed the main bands of the conducting polymer with local maxima at 1541 cm^{-1} (C–C stretching vibrations in the pyrrole ring), 1437 cm^{-1} (C–N stretching vibrations in the ring), 1300 cm^{-1} (C–H or C–N in-plane deformation modes), 1159 and 1092 cm^{-1} (breathing vibrations of the pyrrole rings), and at 1034 and 920 cm^{-1} (C–H and N–H in-plane deformation vibrations). They were shifted only slightly in comparison to the spectrum of polypyrrole powder [31,32]. We also detected a sharp peak of underlying melamine sponge at 807 cm^{-1}.

After heating to 400 °C in inert atmosphere, the spectra of both samples gradually transformed into the spectra of carbon-like materials with two broad bands observed with maxima at 1536 cm^{-1} and 1230 cm^{-1} [14]. The sharp peak of the melamine sponge at 807 cm^{-1} remained at the same position. Above 400 °C, however, any shift of this peak observed for neat melamine (Figure 7a) was overridden by the spectral features of the carbonized polypyrrole coating (Figure 7b,c).

3.6. Raman Spectroscopy

Raman spectra supported the results obtained by infrared spectroscopy. The spectrum of neat melamine sponge (M) recorded with a 780 nm laser excitation at the ambient temperature showed bands with maxima at 1552, 1436, and 1348 cm^{-1}, and a sharp peak at 975 cm^{-1} (Figure 8a). They were transformed into two broad bands with maxima at 1573 and 1328 cm^{-1} at a temperature of 300 °C, and later at 600 and 700 °C. It was found that melamine was thermally stable and the first decomposition changes occurred only at 400 °C (Figure 3).

The structural transformation of melamine sponge was detected at an intermediate temperature of 500 °C, when the spectrum became flat with a fluorescence background and a weak peak at 975 cm^{-1} (Figure 8a). At this temperature, the transformation from melamine sponge to the carbon-like material was in progress. Vibrational spectroscopy (both infrared and Raman) reflect the energy of vibrations of molecular bonds in the sample. The bonds characteristic of melamine were broken, and the corresponding bands disappeared at this temperature range. The new carbon-like bonding was formed at a higher temperature and new bands thus appeared in the spectrum. This interpretation is supported by the sudden decrease observed in the conductivity of the corresponding polypyrrole-coated melamine sponge (cf. Section 3.9 below).

The energy of the laser excitation wavelength 780 nm is in resonance with the energy of delocalized polarons and bipolarons in polypyrrole salt [29]. Because of this, in the Raman spectrum of the melamine sponge coated with 8.2 wt% polypyrrole (Figure 8b), we mainly observed the bands of polypyrrole with local maxima at 1590 cm^{-1} (C=C stretching vibrations of polypyrrole backbone), a maximum at 1486 cm^{-1}, two bands of ring-stretching vibrations at 1386 and 1312 cm^{-1} (the intensity of the latter increased after deprotonation), a band at 1242 cm^{-1} (antisymmetric C–H deformation vibrations), and a double peak with local maxima at 1080 and 1048 cm^{-1} (C–H out-of-plane deformation vibrations, the second one became sharper with deprotonation) [33]. The bands were more profound and slightly shifted with higher polypyrrole content (Figure 8c).

After heating to 400 °C, the Raman spectrum of the melamine sponge with 8.2 wt% PPy was flat (Figure 8b). The spectrum with 27.4 wt% polypyrrole had a shape typical of carbon-like materials (with two broad bands with maxima at 1547 cm^{-1} and 1312 cm^{-1}) with some weak bands at 1040, 975, and 933 cm^{-1} (Figure 8c). For higher temperatures, we observed only two main bands with maxima at 1590 and 1330 cm^{-1}, in the case of 8.2 wt% polypyrrole, and at 1573 and 1335 cm^{-1} for 27.4 wt% polypyrrole. This means that the polypyrrole coating became carbonized.

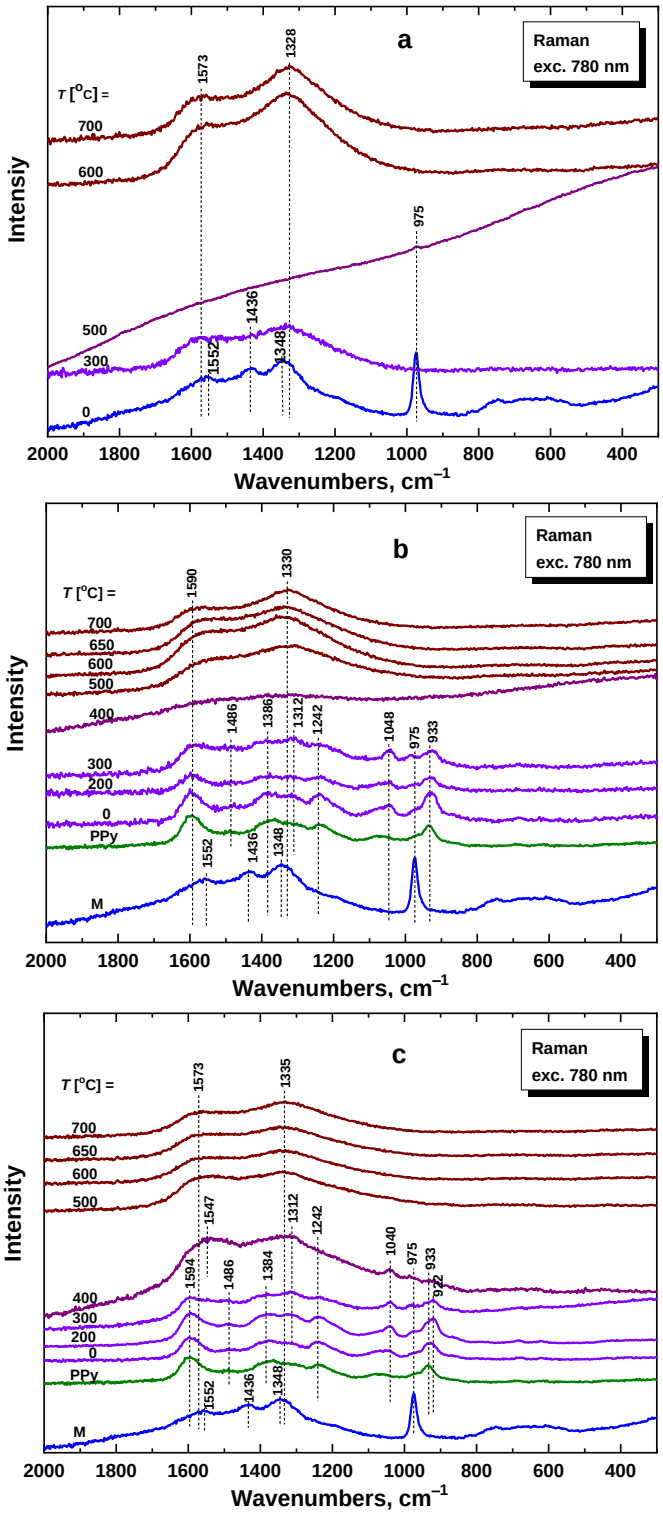

Figure 8. Evolution of the Raman spectra of (**a**) the melamine sponge (M), (**b**) melamine sponge coated with 8.2 wt%, and (**c**) 27.4 wt% polypyrrole, after exposure to various temperatures in inert atmosphere. Laser excitation line was 780 nm. Polypyrrole (PPy) spectrum is included for comparison. The groups of similar spectra are distinguished by colours.

3.7. Surface Properties

The specific surface area is an important parameter for applications of carbons in supercapacitor electrodes or as adsorbents. High specific surface area and enhanced porosity are key parameters required by energy-storage devices in addition to their conductivity.

As expected, the specific surface area increased with increasing temperature to which the sponges were exposed (Figure 9a), and to a greater extent for the sponges with higher polypyrrole content. Similar trends applied to the porosity (Figure 9b). In the absence of polypyrrole and with low polypyrrole content, the evolution of the surface properties during carbonization was similar and basically corresponded to melamine. With higher polypyrrole content, the specific surface area was determined especially by polypyrrole deposited on the melamine threads. The specific surface area increased and passed through a maximum. Decrease in the surface area polypyrrole after exposure to the highest temperature has also been observed for globular polypyrrole alone [14], associated with continuing changes in the molecular structure. These results suggest that the present carbonaceous materials may be good candidates for use in applications such as supercapacitors.

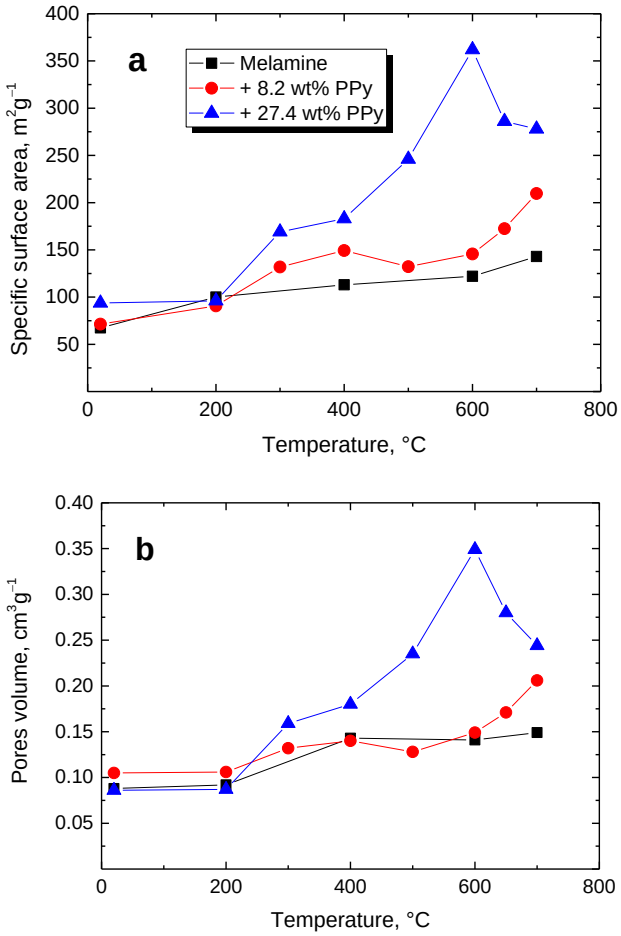

Figure 9. (**a**) Specific surface area, and (**b**) pores volume of the sponges after exposure to various temperatures.

3.8. Mechanical Properties

While properties such as specific surface area, porosity, and conductivity are of importance for various applications, the materials' properties are equally, or even more, important. The method of conductivity determination in the present experimental setup (Figure 1) also enabled information to be obtained on mechanical properties by plotting sample thickness against applied pressure.

The dependence of the sample thickness d on the applied pressure p was nearly linear in the double-logarithmic presentation, i.e., it can be represented by the simple relation $d = A\ p^{-B}$, where the parameter A is the sample thickness at 1 MPa pressure (original thickness at a "zero" pressure is approximately 1 cm for all samples) and the parameter B is the logarithmic change in the sample thickness per pressure decade (Table 1). The

former parameter A can be regarded as a measure of "rigidity", i.e., how much is the sample size reduced from 1 cm after application of 1 MPa pressure—the lower the value after compression, the less rigid the structure. The latter parameter B is a measure of compressibility—the higher the value, the more easily the sample is compressed. When we exclude the initial poorly defined range of low pressures (<0.05 MPa), the double-logarithmic curves were slightly concave and the parameter B had a higher value at low pressures. The sample was more easily deformed than at higher pressures, where the same logarithmic pressure difference resulted in a lower deformation. The results are only qualitative because the initial sample thickness at a "zero" pressure varied somewhat for individual samples, but the trends are obvious.

Table 1. Mechanical rigidity A and compressibility B (at low to high pressure) of melamine sponge coated with 27.4 wt% polypyrrole and exposed to various temperatures [a].

Temperature (°C)	Rigidity, A (cm MPa^B)	Compressibility, B
20	0.124	0.51–0.40
200	0.130	0.53–0.40
300	0.080	0.62–0.33
400	0.073	0.57–0.37
500	0.067	0.64–0.42
600	0.055	0.64–0.44
650	0.055	0.63–0.47
700	(b)	0.71–0.49

[a] Based on the data depicted in Figure 10. [b] Below the apparatus limit of thickness, 0.04 cm.

The present results refer to a single compression test. The behavior was elastic in the low-pressure region, suggesting the samples could be used as pressure sensors with good recovery [34]. Under high pressures, however, the deformation became plastic and the sample deformation was not fully reversible. This fact needs to be borne in mind in consideration of the electrical properties.

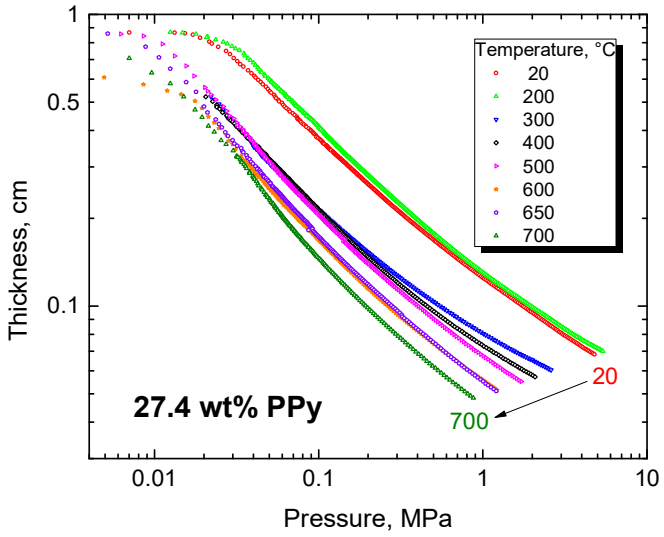

Figure 10. Dependence of the sample thickness on the applied pressure for polypyrrole-coated sponges after exposure to elevated temperatures.

3.9. Conductivity

The resistivity was determined by the four-point van der Pauw method (cf. Experimental Methods) during compression from pressure of approximately 0.01 up to 1 MPa. As the pressure increased, the thickness of the sample decreased. In the double-logarithmic presentation, when resistivity is plotted against sample thickness, the curves are close to

straight lines with approximately the same slope, regardless of the carbonization temperature, and even of polypyrrole content (Figure 11a,b). The dependence for the sample treated at 400 °C is missing in Figure 11a because the resistivity was too high to be determined using the present experimental setup.

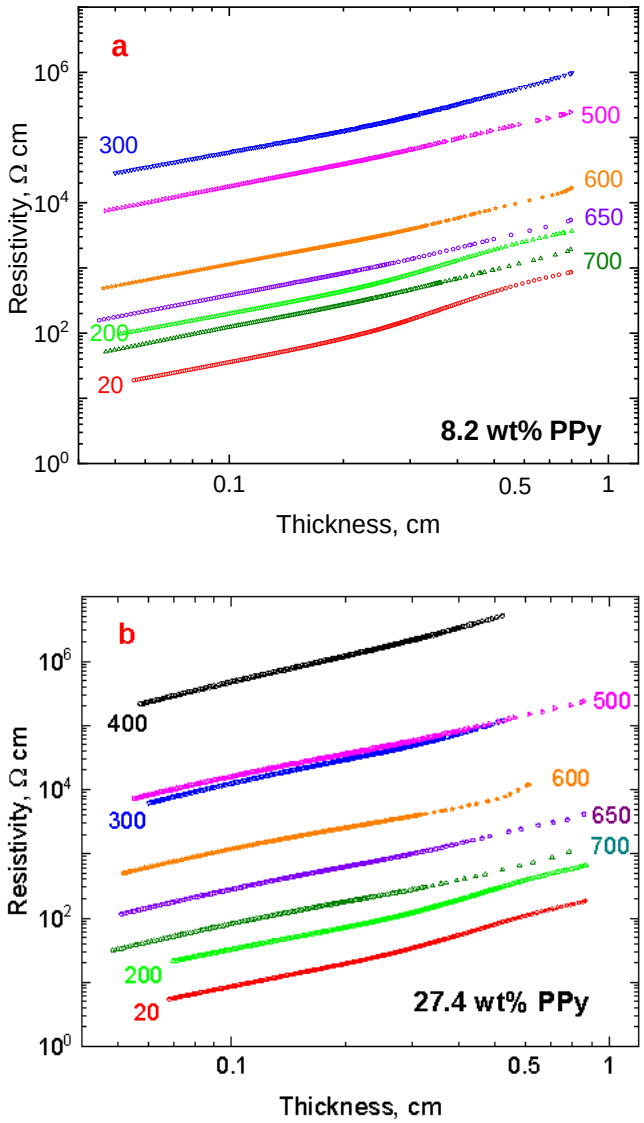

Figure 11. Resistivity of polypyrrole-coated sponges exposed to various temperatures 20–700 °C on the sample thickness during compression at 0.04–1 MPa pressure. Polypyrrole content (**a**) 8.2 wt%, and (**b**) 27.4 wt%.

When the results are plotted in terms of the conductivity determined at fixed 0.1 MPa pressure (Figure 12), a drop in the conductivity due to polypyrrole deprotonation was observed [29] followed by decomposition at close to 400 °C, and then by recovery of conductivity due to carbonization in the course of temperature increase to 700 °C. Based on the above spectroscopic analysis of molecular structure, the following explanation is suggested: During the deprotonation associated with the loss of hydrochloric acid (Figure 1b), the number of charge carriers represented by cation radicals (polarons) on polypyrrole chains becomes reduced. The chain conjugation, i.e., the alternation of single and double bonds in polypyrrole, is damaged and, consequently, conducting pathways are broken. Both effects result in the decrease of conductivity at 400 °C. The conjugated

structure recovers during the graphitization by generation of new double bonds at higher carbonization temperature with consequent increase in the conductivity.

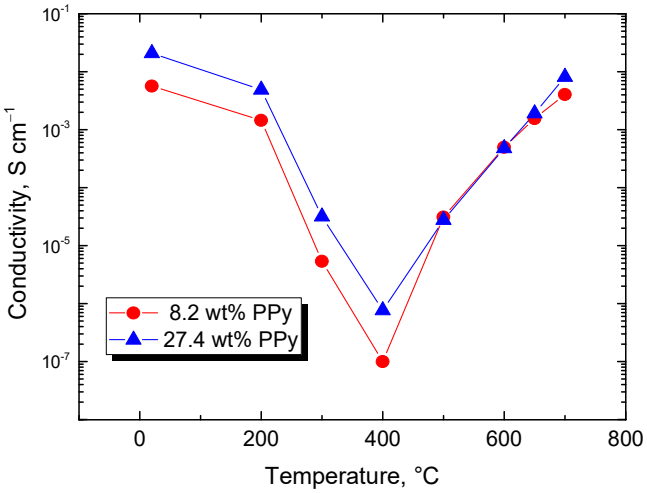

Figure 12. Conductivity of the polypyrrole-coated sponge exposed to various temperatures determined at 0.1 MPa pressure. The low conductivity of sponge with 8.2 wt% polypyrrole exposed to 400 °C was estimated separately by a two-point method.

3.10. Electromagnetic Radiation Shielding

Electromagnetic radiation shielding is one of the many applications of conducting polymers [35] where the low apparent density of sponge-like materials is especially valued. The reduction of radiation transmission in the MHz–GHz frequency region is at the expense of increased radiation absorption and reflection. Conducting polymers, and their composites, afford both radiation absorption and, to a lesser extent, reflection, which are, in the first approximation, proportional to the conductivity of the material [27,36,37]. The 1–12 GHz frequency range is important, since the majority of communication and information transfer systems use it for operation.

The radiation shielding afforded by polypyrrole-modified sponges was practically independent of frequency in the range 8.2–12.4 GHz (Figure 13). For that reason, only the data obtained at 9 GHz are reported below.

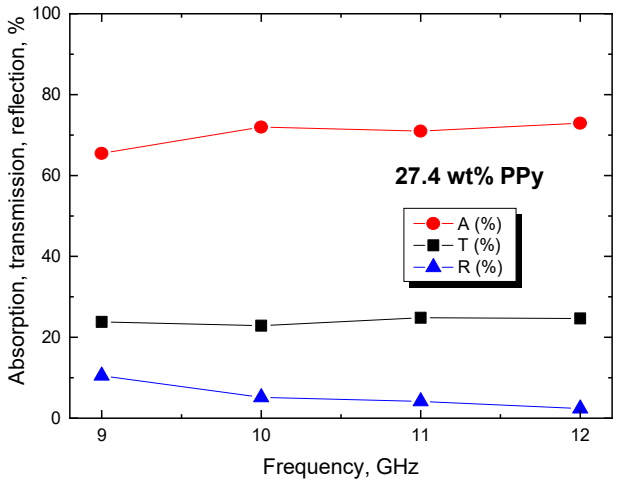

Figure 13. Radiation frequency dependence of absorption, transmission and reflection contributions tested on the original sponge containing 27.4 wt% polypyrrole.

By comparing the shielding contributions (Figure 14) with the conductivity (Figure 11), the qualitative correlation between these quantities was obvious. This applied especially

to the radiation absorption, which was higher than the reflected component. Radiation shielding was negligible for the sponge with a low 8.2 wt% polypyrrole content, when the transmission fraction was close to 100% and only for a fully carbonized sample did a shielding effect start to be observable (Figure 14a).

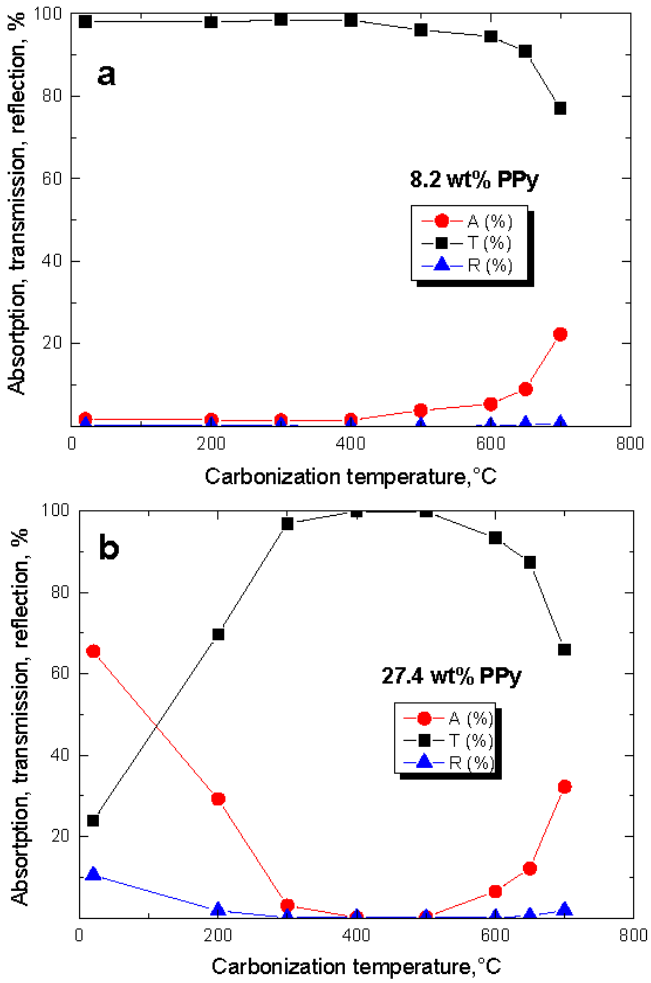

Figure 14. Absorption, transmission and reflection contributions of the 9 GHz radiation for the sponges containing (**a**) 8.2 wt%, or (**b**) 27.4 wt% polypyrrole.

The effect of higher conductivity manifested itself in reasonable absorption by the original sponges with a higher polypyrrole content, 27.4 wt% (Figure 14b). It decreased to zero as the carbonization temperature reached 400–500 °C and the conductivity dropped (Figure 11). The absorption of radiation recovered at still higher carbonization temperatures in accordance with the increase in conductivity. The radiation reflection followed the same pattern, but its contribution was significantly lower than that of the absorption.

The conductivity, however, is not the sole parameter that controls shielding efficiency. Changes in the molecular structure and surface properties occurring during carbonization are also likely to affect, for instance, multiple internal reflections, and thus to contribute to radiation shielding.

4. Conclusions

This report considered the design of new macroporous organic materials rich in carbon and nitrogen with good conductivity, high specific surface area and sponge-like mechanical properties. Macroporous open-cell melamine sponge can be easily coated with a conducting polymer, polypyrrole, here at 8.2 and 27.4 wt% content. When exposed to elevated temperature, the original conductivity of polypyrrole-coated sponges of the

order 10^{-2}–10^{-3} S·cm^{-1} was initially reduced, then almost effectively lost at 400 °C, but recovered close to its original level as the material converted to a nitrogen-containing carbon at 650–700 °C. The specific surface area and porosity increased at the same time. The carbon content increased to ca. 60 wt% after carbonization, but still held a reasonable amount of nitrogen, 10–20 wt%. The products were, thus, macroporous nitrogen-containing carbons with good conductivity and mechanical properties. The sponges were elastic under low pressures with good recovery after release but became irreversibly compressed under high pressures. They could be applied, for example, as moderate-pressure sensors, porous electrodes in supercapacitors and in electrocatalysis, for steam generation, as heating elements, or in the controlled adsorption of pollutant dyes, etc. [31,35]. Electromagnetic radiation shielding by polypyrrole-coated sponges is an example of another application. This suggestion is based on the radiation absorption, which was controlled mainly by the sample conductivity and, consequently, was proportional to the polypyrrole loading. The contribution of radiation reflection followed the same pattern but was much lower compared to the absorption.

Author Contributions: J.S.: conceptualization, writing—original draft, funding acquisition; J.V.: supervision, project administration, investigation, methodology; M.J.: investigation; H.F.: investigation; M.T.: data curation, writing—review and editing; Z.K.: data curation, formal analysis; J.P.: investigation, data curation; I.K.: data curation, software. All authors have read and agreed to the published version of the manuscript.

Funding: This work was supported by the Ministry of Education, Youth and Sports of the Czech Republic (DKRVO (RP/CPC/2020/005)) and M-era.Net project "LiBASED Li-ion BAttery-SupErcapacitor hybrid Device" co-funded by the Technology Agency of the Czech Republic (Epsilon TH71020006).

Institutional Review Board Statement: Not applicable.

Informed Consent Statement: Not applicable.

Data Availability Statement: The authors confirm that the data supporting the findings of this study are available within the article.

Conflicts of Interest: The authors declare no conflict of interest.

References

1. Feng, Y.; Yao, J.F. Design of melamine sponge-based three-dimensional porous materials toward applications. *Ind. Eng. Chem. Res.* **2018**, *57*, 7322–7330. [CrossRef]
2. Chen, S.L.; He, G.H.; Hu, H.; Jin, S.Q.; Zhou, Y.; He, Y.Y.; He, S.J.; Zhao, F.; Hou, H.Q. Elastic carbon foam via direct carbonization of polymer foam for flexible electrodes and organic chemical absorption. *Energy Environ. Sci.* **2013**, *6*, 2435–2439. [CrossRef]
3. Ghani, M.; Maya, F.; Cerdà, V. Automated solid-phase extraction of organic pollutants using melamine-formaldehyde polymer-derived carbon foams. *RSC Adv.* **2016**, *6*, 48558–48565. [CrossRef]
4. Jing, X.X.; Kang, W.J.; Wang, L.; Wei, D.H.; Qu, K.G.; Li, R.; Chen, B.L.; Guo, Z.J.; Li, H.B. Regulating capacitative performance of monolithic carbon sponges by balancing heteroatom content, surface area and graphitization degree. *ChemNanoMat* **2020**, *6*, 1507–1512. [CrossRef]
5. Shi, Y.N.; Pan, K.C.; Moloney, M.G.; Qiu, J. Strain sensing nanocomposites of polyaniline–silver nanoparticles/carbon foam. *Composites A* **2021**, *144*, 106351. [CrossRef]
6. Trchová, M.; Konyushenko, E.N.; Stejskal, J.; Kovářová, J.; Ćirić-Marjanović, G. The conversion of polyaniline nanotubes to nitrogen-containing carbon nanotubes and their comparison with multi-walled carbon nanotubes. *Polym. Degrad. Stabil.* **2009**, *94*, 929–938. [CrossRef]
7. Ismael, M. A review on graphitic carbon nitride (g-C_3N_4) based nanocomposites: Synthesis, categories, and their application in photocatalysis. *J. Alloys Compd.* **2020**, *846*, 156446. [CrossRef]
8. Stolz, A.; Le Floch, S.; Reinert, L.; Ramos, S.M.M.; Tuaillon-Combes, J.; Soneda, Y.; Chaudet, P.; Baillis, D.; Blanchard, N.; Duclaux, L.; et al. Melamine-derived carbon sponges for oil-water separation. *Carbon* **2016**, *107*, 198–208. [CrossRef]
9. Lei, Z.W.; Zheng, P.T.; Niu, L.Y.; Yang, Y.; Shen, J.L.; Zhang, W.D.; Wang, C.Y. Ultralight, robustly compressible and superhydrophobic biomass-decorated carbonaceous melamine sponge for oil/water separation with high oil retention. *Appl. Surf. Sci.* **2019**, *489*, 922–929. [CrossRef]
10. Zhang, R.; Jing, X.X.; Chu, Y.T.; Wang, L.; Kang, W.J.; Wei, D.H.; Li, H.B.; Xiong, S.L. Nitrogen/oxygen co-doped monolithic carbon electrodes derived from melamine foam for high-performance supercapacitors. *J. Mater. Chem. A* **2018**, *6*, 17730–17739. [CrossRef]

11. Cao, M.J.; Feng, Y.; Tian, R.R.; Chen, Q.; Chen, J.H.; Jia, M.M.; Yao, J.F. Free-standing porous carbon foam as the ultralight and flexible supercapacitor electrode. *Carbon* **2020**, *161*, 224–230. [CrossRef]
12. Zhang, X.Q.; Le, H.; Qing, Y.; Gao, Z.F.; Wu, Y.Q.; Hu, S.H.; Xia, L.Y. Fabrication of robust, highly conductive, and elastic hybrid carbon foam platform for high-performance compressible asymmetry supercapacitors. *ACS Omega* **2021**, *6*, 14230–14241. [CrossRef] [PubMed]
13. Ćirić-Marjanović, G.; Pašti, I.; Gavrilov, N.; Janosević, A.; Mentus, S. Carbonised polyaniline and polypyrrole: Towards advanced nitrogen-containing carbon materials. *Chem. Pap.* **2013**, *67*, 781–813. [CrossRef]
14. Stejskal, J.; Kohl, M.; Trchová, M.; Kolská, Z.; Pekárek, M.; Křivka, I.; Prokeš, J. Conversion of conducting polypyrrole nanostructures to nitrogen-containing carbons and its impact on the adsorption of organic dye. *Mater. Adv.* **2021**, *2*, 706–717. [CrossRef]
15. Kopecká, J.; Mrlík, M.; Olejník, R.; Kopecký, D.; Vrňata, M.; Prokeš, J.; Bober, P.; Morávková, Z.; Trchová, M.; Stejskal, J. Polypyrrole nanotubes and their carbonized analogs: Synthesis, characterization, gas sensing properties. *Sensors* **2016**, *16*, 1917. [CrossRef]
16. Elyashevich, G.K.; Rosova, E.Y.; Andreeva, D.V.; Polotskaya, G.A.; Trchová, M.; Pientka, Z. New composite systems on the base of polyethylene porous films covered by polypyrrole and polyacrylic acid. *J. Appl. Polym. Sci.* **2005**, *97*, 1410–1417. [CrossRef]
17. Smirnov, M.A.; Kuryndin, I.S.; Nikitin, L.N.; Sidorovich, A.V.; Sazanov, Y.N.; Kudasheva, O.V.; Bukosek, V.; Khokhlov, A.R.; Elyashevich, G.K. Properties of conducting composite systems containing polypyrrole layers on porous polyethylene films. *Russ. J. Appl. Chem.* **2005**, *78*, 1993–2001. [CrossRef]
18. Elyashevich, G.K.; Dmitriev, I.Y.; Rozova, E.Y. Electroconducting polypyrrole coatings as an electrode contact material on porous poly(vinylidene fluoride) piezofilm. *Polym. Sci. A* **2021**, *63*, 45–53. [CrossRef]
19. Hermenegildo, B.; Ribeiro, C.; Peřinka, N.; Martins, V.; Trchová, M.; Hajná, M.; Stejskal, J.; Lanceros-Méndez, S. Electroactive poly(vinylidene fluoride) electrospun fiber mats with polyaniline and polypyrrole for tissue regeneration applications. *React. Funct. Polym.* **2022**, *170*, 105116. [CrossRef]
20. Meng, K.; Ding, K.; Wang, Y.B. A superhydrophobic sponge with hierarchical structure as an efficient and recyclable oil absorbent. *ChemPlusChem* **2015**, *80*, 1435–1439. [CrossRef]
21. Gao, Z.Y.; Zhang, L.C.; Chang, J.L.; Wang, Z.; Wu, D.P.; Xu, F.; Guo, Y.M.; Jiang, K. Catalytic electrode-redox electrolyte supercapacitor system with enhanced capacitive performance. *Chem. Eng. J.* **2018**, *335*, 590–599. [CrossRef]
22. Qi, L.; Gong, J.C. Facile in-situ polymerization of polyaniline-functionalized melamine sponge preparation for mass spectrometric monitoring of perfluorooctanoic acid and perfluorooctane sulfonate from biological samples. *J. Chromatogr. A* **2020**, *1616*, 460777. [CrossRef]
23. Li, L.; Wang, K.; Huang, Z.Q.; Zhang, C.; Liu, T.X. Highly ordered graphene architectures by duplicating melamine sponges as a three-dimensional deformation-tolerant electrode. *Nano Res.* **2016**, *9*, 2938–2949. [CrossRef]
24. Chang, Y.H.; Wang, N.; Han, G.Y.; Li, M.Y.; Xiao, Y.M.; Li, H.G. The properties of highly compressible electrochemical capacitors based on polypyrrole/melamine sponge-carbon fibers. *J. Alloys Compd.* **2019**, *786*, 668–676. [CrossRef]
25. Xu, M.; Ma, Y.; Liu, R.; Liu, Y.; Bai, Y.; Wang, X.; Huang, Y.Y.; Yuan, G.H. Melamine sponge modified by graphene/polypyrrole as highly compressible supercapacitor electrodes. *Synth. Met.* **2020**, *267*, 116461. [CrossRef]
26. Wu, X.W.; Lei, Y.G.; Li, S.H.; Huang, J.Y.; Teng, L.; Chen, Z.; Lai, Y.K. Photothermal and Joule heating-assisted thermal management sponge for efficient cleanup of highly viscous crude oil. *J. Hazard. Mater.* **2021**, *403*, 124090. [CrossRef]
27. Stejskal, J.; Sapurina, I.; Vilčáková, J.; Jurča, M.; Trchová, M.; Kolská, Z.; Prokeš, J.; Křivka, I. One-pot preparation of conducting melamine/polypyrrole/magnetite ferrosponge. *ACS Appl. Polym. Mater.* **2021**, *3*, 1107–1115. [CrossRef]
28. Guo, Y.F.; Su, J.P.; Yang, H.; Gu, F.L.; Song, Y.H.; Zhu, Y.M. Flexible foam carbon/graphene oxide/Schiff base polymer-derived carbon/polyaniline for high-performance supercapacitor. *Ionics* **2021**, *27*, 2639–2647. [CrossRef]
29. Stejskal, J.; Trchová, M.; Bober, P.; Morávková, Z.; Kopecký, D.; Vrňata, M.; Prokeš, J.; Varga, M.; Watzlová, E. Polypyrrole salts and bases: Superior conductivity of nanotubes and their stability towards the loss of conductivity by deprotonation. *RSC Adv.* **2016**, *6*, 88382–88391. [CrossRef]
30. Stejskal, J.; Sapurina, I.; Vilčáková, J.; Humpolíček, P.; Truong, T.H.; Shishov, M.A.; Trchová, M.; Kopecký, D.; Kolská, Z.; Prokeš, J.; et al. Conducting polypyrrole-coated macroporous melamine sponges: A simple toy or an advanced material? *Chem. Pap.* **2021**, *75*, 5035–5055. [CrossRef]
31. Stejskal, J.; Trchová, M. Conducting polypyrrole nanotubes: A review. *Chem. Pap.* **2018**, *72*, 1563–1595. [CrossRef]
32. Stejskal, J.; Trchová, M.; Lapčák, L.; Kolská, Z.; Kohl, M.; Pekárek, M.; Prokeš, J. Comparison of carbonized and activated polypyrrole globules, nanofibers, and nanotubes as conducting nanomaterials and adsorbents of organic dye. *Carbon Trends* **2021**, *4*, 100068. [CrossRef]
33. Stejskal, J.; Trchová, M.; Bober, P.; Humpolíček, P.; Kašpárková, V.; Sapurina, I.; Shishov, M.A.; Varga, M. Conducting Polymers: Polyaniline. In *Encyclopedia of Polymer Science and Technology*; Wiley Online Library: Hoboken, NJ, USA, 2015; pp. 1–44. [CrossRef]
34. Stejskal, J.; Trchová, M.; Kasparyan, H.; Kopecký, D.; Kolská, Z.; Prokeš, J.; Křivka, I.; Vajďák, J.; Humpolíček, P. Pressure-sensitive conducting and antibacterial materials obtained by in situ dispersion coating of macroporous melamine sponges with polypyrrole. *ACS Omega* **2021**, *6*, 20895–20901. [CrossRef]
35. Stejskal, J. Conducting polymers are not just conducting: A perspective for emerging technology. *Polym. Int.* **2020**, *62*, 662–664. [CrossRef]

36. Wang, Y.Y.; Jing, X.L. Intrisinsically conducting polymers for electromagnetic interference shielding. *Polym. Adv. Technol.* **2005**, *16*, 344–351. [CrossRef]
37. Das, N.C.; Yamazaki, S.; Hikosaka, M.; Chaki, T.K.; Khastgir, D.; Chakraborty, A. Electrical conductivity and electromagnetic shielding effectiveness of polyaniline–ethylene vinyl acetate composites. *Polym. Int.* **2005**, *54*, 256–259. [CrossRef]